Eur. Phys. J. B **12**, 209–216 (1999)

THE EUROPEAN PHYSICAL JOURNAL B

EDP Sciences

Optimum ground states of generalized Hubbard models with next-nearest neighbour interaction*

C. Dziurzik, A. Schadschneider[a], and J. Zittartz

Institut für Theoretische Physik, Universität zu Köln, Zülpicher Strasse 77, 50937 Köln, Germany

Received 30 March 1999 and Received in final form 3 May 1999

Abstract. We investigate the stability domains of ground states of generalized Hubbard models with next-nearest neighbour interaction using the optimum groundstate approach. We focus on the η-pairing state with momentum $P = 0$ and the fully polarized ferromagnetic state at half-filling. For these states exact lower bounds for the regions of stability are obtained in the form of inequalities between the interaction parameters. For the model with only nearest neighbour interaction we show that the bounds for the stability regions can be improved by considering larger clusters. Additional next-nearest neighbour interactions can lead to larger or smaller stability regions depending on the parameter values.

PACS. 75.10.Lp Band and itinerant models – 74.20.-z Theories and models of superconducting state

1 Introduction

Correlation effects are of great importance in condensed matter physics. Superconductivity and ferromagnetism are two important phenomena which can arise in an interacting many-body system. Theoretical investigations usually begin with choosing a suitable Hamiltonian. In general this Hamiltonian is too complex and must be reduced to a reasonable model which gives only a simplified description of reality. Such simplifications make it even more desirable to obtain exact results and compare these with experimental data. In addition, they can be used to check the results from computer simulations and approximative methods.

The simplest model of correlated electrons was introduced independently by Hubbard, Gutzwiller and Kanamori in 1963 as an attempt to describe the effect of correlations for d-electrons in transition metals [1–3]. This model consists of two terms, one describes discrete quantum mechanical motion of electrons (*hopping*) and the other one the *on-site* Coulomb interaction between electrons. Nevertheless, the *Hubbard model* is one of the most important models in theoretical physics and is believed to exhibit various phenomena including metal-insulator transition, ferromagnetism, antiferromagnetism and superconductivity. In spite of its simplicity only a few exact results are known. For instance, Lieb and Wu solved the one-dimensional ($D = 1$) model by using *Bethe-Ansatz*-technique [4]. The other class of exact solutions belongs to the limiting case $D = \infty$, where a dynamical mean-field approximation becomes exact [5,6]. However, the situation becomes much more complicated in the lower dimensional cases.

In recent years a new, non-pertubative method was developed by Brandt and Giesekus [7]. The main idea is to start with a well-known ground state and then construct a corresponding Hamiltonian in the form of a projection operator. This approach permits to include a large class of interaction parameters. A generalization of this method was presented by Strack and Vollhardt [8,9]. Ovchinnikov improved some of the results obtained previously by using a different method [10] (see also [11]). His approach is based on *Gerschgorin's theorem* which gives a lower bound for the ground state energy of the Hamiltonian and thus complements the usual variational principle which gives upper bounds. A much simpler and clearer method was used by de Boer and Schadschneider [12]. This method is called *Optimum Groundstate Approach* and was introduced by Klümper, Schadschneider and Zittartz for spin models [13]. The basic idea is to diagonalize a specially chosen local Hamiltonian and to make all the local states which are needed for the construction of a given global ground state also local ground states by choosing the interaction parameters appropriately. This approach leads to some inequalities between the interaction parameters which represent the minimal stability region of the investigated ground state. Due to this restriction only a subspace of the parameter space can be examined.

Using a larger local Hamiltonian enables in a natural way the inclusion of more interactions which determine the stability conditions. In general, one finds an extension of the stability domain of the ground state. Independently, Szabó took this into account and improved some results obtained previously [14]. Additionally, he examined the behaviour of the stability domain in the presence of next-nearest neighbour interaction parameters. For instance, in the case of η-pairing state with momentum $P = \pi$ he verified a shrinking of the stability region for a small ratio

* Work performed within the research program of the Sonderforschungsbereich 341 (Köln-Aachen-Jülich)

[a] e-mail: as@thp.uni-koeln.de

between nearest and next-nearest neighbour hopping. In contrast to his numerical approach we shall investigate various ground states using analytical calculations.

2 Method

A Hamiltonian of a many-body system on an arbitrary lattice but with homogeneous α-nearest neighbour interaction can be split up into local Hamiltonians, *e.g.* $H = \sum_{\square} h_{\square}$. The minimal cluster $\square$ consists of only two nearest ($\alpha = 1$) neighbour lattice sites $\langle ij \rangle$ and the corresponding local Hamiltonian is called *bond* Hamiltonian. The largest cluster contains obviously all lattice sites and can be expressed by $h_{\square} = H$. For small clusters $\square$ the local Hamiltonian $h_{\square}$ can be diagonalized exactly. This limits the tractable cluster size. By adding a trivial constant to the Hamiltonian H, which never changes the physics, one can achieve that the lowest eigenvalue e_0 of $h_{\square}$ vanishes, *i.e.* $e_0 = 0$. In this case the lowest eigenvalue E_0 of H is either positive ($E_0 > 0$) or zero ($E_0 = 0$), because $h_{\square}$ is a positive-semidefinite operator and the sum of such operators is also positive semidefinite. In the special case $E_0 = 0$ a local condition for finding a ground state $|\Psi_0\rangle$ exists:

$$H|\Psi_0\rangle = 0 \quad \Longleftrightarrow \quad h_{\square}|\Psi_0\rangle = 0 \qquad (\text{for all} \quad \square). \tag{1}$$

This equivalence can be understood by considering $\sum_{\square} \langle \Psi_0 | h_{\square} | \Psi_0 \rangle = \langle \Psi_0 | H | \Psi_0 \rangle = 0$. Since the $h_{\square}$ are positive-semidefinite, all $\langle \Psi_0 | h_{\square} | \Psi_0 \rangle$ must vanish, which in turn implies (1). In the case $E_0 = 0$, the global ground state consists only of ground states of the local Hamiltonian and no excited local states are involved. A ground state of this type is called *optimum ground state*. To obtain such ground states for a given system one must perform two steps. First, the ground states of the local Hamiltonian must be determined. Then one has to check whether a global ground state can be formed using only these local ground states.

3 The generalized Hubbard model

The Hamiltonian of the generalized Hubbard-Model on a D-dimensional, hypercubic lattice with L sites and homogeneous α-nearest neighbour interaction can be split up into local Hamiltonians $h_{ij}^{(\alpha)}$. Due to homogeneity all local Hamiltonians are equal and can be divided into two parts. The first part contains hopping and interaction terms:

$$\begin{aligned} h_{ij}^{(\alpha)} = & -t_\alpha \sum_\sigma (\hat{c}_{i\sigma}^\dagger \hat{c}_{j\sigma} + \hat{c}_{j\sigma}^\dagger \hat{c}_{i\sigma}) \\ & + X_\alpha \sum_\sigma (\hat{c}_{i\sigma}^\dagger \hat{c}_{j\sigma} + \hat{c}_{j\sigma}^\dagger \hat{c}_{i\sigma})(\hat{n}_{i,-\sigma} + \hat{n}_{j,-\sigma}) \\ & + Y_\alpha (\hat{c}_{i\uparrow}^\dagger \hat{c}_{i\downarrow}^\dagger \hat{c}_{j\downarrow} \hat{c}_{j\uparrow} + \hat{c}_{j\uparrow}^\dagger \hat{c}_{j\downarrow}^\dagger \hat{c}_{i\downarrow} \hat{c}_{i\uparrow}) \\ & + \frac{J_\alpha^{xy}}{2} (\hat{S}_i^+ \hat{S}_j^- + \hat{S}_j^+ \hat{S}_i^-) + J_\alpha^z \hat{S}_i^z \hat{S}_j^z \\ & + V_\alpha (\hat{n}_i - 1)(\hat{n}_j - 1), \end{aligned} \tag{2}$$

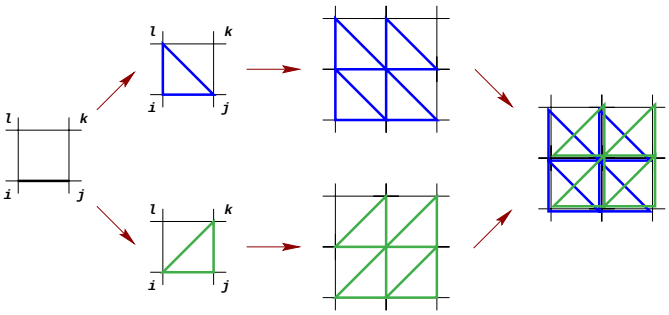

Fig. 1. Covering of 3-site clusters on a square lattice. In order to obtain the full lattice including next-nearest neighbour interaction (diagonal bonds) one has to cover the lattice with two different 3-site clusters, namely triangle of type "lij" (upper part) and "ijk" (lower part).

where the pairs (ij) denote α-nearest neighbours, for instance nearest ($\alpha = 1$) and next-nearest ($\alpha = 2$) neighbours. The fermion operators $\hat{c}_{i\sigma}^\dagger$ and $\hat{c}_{i\sigma}$ create and annihilate electrons with spin $\sigma \in \{\uparrow, \downarrow\}$ at site i which is associated with the single tight-binding Wannier orbital. The corresponding number operators are $\hat{n}_{i\sigma} = \hat{c}_{i\sigma}^\dagger \hat{c}_{i\sigma}$ and $\hat{n}_i = \hat{n}_{i\uparrow} + \hat{n}_{i\downarrow}$. The $SU(2)$ spin operators are given by $\hat{S}_i^z = (\hat{n}_{i\uparrow} - \hat{n}_{i\downarrow})/2$, $\hat{S}_i^- = \hat{c}_{i\downarrow}^\dagger \hat{c}_{i\uparrow}$ and $\hat{S}_i^+ = \hat{c}_{i\uparrow}^\dagger \hat{c}_{i\downarrow}$. The physical nature of the various terms is as follows: The first term (t) is the usual hopping of fermions on a lattice. The next two terms, bond-charge interaction (X) and pair-hopping (Y), were studied in relation with superconductivity [15–17]. The fourth term is an anisotropic Heisenberg term with a XXZ-type spin interaction given by the exchange constants J^{xy} and J^z. The last term (V) is known as the α-nearest neighbour Coulomb interaction. Estimates for the values of the couplings (for metals) for example can already be found in Hubbard's original paper [1].

The second term contains only on-site interactions $O_{ij} = O_i + O_j$ with

$$O_i = \frac{U}{Z}(\hat{n}_{i\uparrow} - 1/2)(\hat{n}_{i\downarrow} - 1/2) + \frac{\mu}{Z}\hat{n}_i. \tag{3}$$

Here U is the on-site Coulomb interaction, μ the chemical potential and Z the coordination number of nearest neighbour sites on the D-dimensional hypercubic lattice. A local Hamiltonian $h_{\square}$ can be divided into bond Hamiltonians such that a comparison with the results obtained in [12] is possible. We restrict our extension to cluster sizes $N(\square) = \{3, 4\}$ and call the corresponding local Hamiltonians 3- and 4-site Hamiltonian. In this case only nearest ($\alpha = 1$) and next-nearest ($\alpha = 2$) neighbour interactions exist on the square lattice and therefore:

$$h_{\square} := \frac{1}{F} \sum_{\langle ij \rangle_1 \in \square} \left(h_{ij}^{(1)} + O_{ij} \right) + \sum_{\langle ij \rangle_2 \in \square} h_{ij}^{(2)}. \tag{4}$$

The factor $F := 2(D-1)$ for $D > 1$ is only necessary in order to compare results of different clusters without rescaling the coupling constants (due to multiple counts of bonds). Figure 1 shows the covering

Table 1. Block sizes and number of blocks for the 3-site Hamiltonian.

$X \neq t$		$X = t$	
number	block size	number	block size
4	1×1	4	1×1
8	3×3	12	3×3
4	9×9	4	6×6

of 3-site clusters on a square lattice. The entries of a local state are described by $\xi \in \{0, \uparrow, \downarrow, 2\}$, where '0' denotes an empty site, $\sigma \in \{\uparrow, \downarrow\}$ a site occupied by one electron with spin σ and '2' a doubly occupied site. The local state of cluster size $N(\square)$ is a tensor product $|\xi_1 \xi_2 \dots \xi_{N(\square)}\rangle = |\xi_1\rangle \otimes |\xi_2\rangle \otimes \dots \otimes |\xi_{N(\square)}\rangle$. Together one gets $4^{N(\square)}$ local states and a $4^{N(\square)} \times 4^{N(\square)}$-matrix which represents the local Hamiltonian. Although this matrix might be very large, the number of zero elements is still a large number. The use of symmetries makes the problem more tractable. One of the simplest symmetries is associated with the conservation of the total number of electrons. One has to consider only subspaces corresponding to a fixed number of electrons, *i.e.* one gets a block diagonal matrix. Another useful condition which we shall frequently impose is $X = t$. It leads to the preservation of the number of doubly occupied sites (see *e.g.* [8,18]) and thus some of the block matrices split into smaller ones. Table 1 summarizes the results for the 3-site Hamiltonian with corresponding 64×64-matrix.

However, the determination of algebraic eigenvalues of a characteristic polynomial $p(\lambda) = \det(\mathbb{M} - \lambda \mathbb{I})$ is limited, *i.e.* only polynomials up to fourth degree can be solved in closed form. In the case $X = t$ it is possible to find a convenient transformation with a corresponding matrix $\mathbb{T}$. After the transformation $\mathbb{T}^{-1}\mathbb{M}\mathbb{T} = \overline{\mathbb{M}}$ the four 6×6-matrices decay into blocks of size 3 and all eigenvalues can be obtained in closed form. This is the main reason why we concentrate here on the case $X = t$.

4 Results

We shall restrict our discussion in the following to two physically interesting classes of states. The first class are the η-pairing states with momentum P which show off-diagonal long-range order (ODLRO) and are thus superconducting [19]. The second one is the fully polarized ferromagnetic state at half-filling. We determine under which circumstances these states are optimum ground states of the generalized Hubbard model. We shall mainly consider the square lattice ($D = 2$).

The definition of an η-pairing state with momentum P is given by the expression

$$|\eta\rangle = \left(\eta_P^\dagger\right)^{\mathcal{N}} |0\rangle \quad \text{with} \quad \eta_P^\dagger = \sum_{j=1}^{L} \mathrm{e}^{\mathrm{i}Pj} \hat{c}_{j\downarrow}^\dagger \hat{c}_{j\uparrow}^\dagger, \qquad (5)$$

where $\mathcal{N}$ is an integer which is related to the particle number N through $\mathcal{N} = N/2$. Since we would like the η-pairing state to be the ground state of the global Hamiltonian it is informative to determine the commutator $[H, \eta_P^\dagger]$. A long, but straightforward calculation yields:

$$\begin{aligned}
[H, \eta_P^\dagger] = &\sum_{\alpha=1}^{2} 2(X_\alpha - t_\alpha) \\
&\times \sum_{\langle jk \rangle_\alpha} \left(\mathrm{e}^{\mathrm{i}Pj} + \mathrm{e}^{\mathrm{i}Pk}\right) (\hat{c}_{j\downarrow}^\dagger \hat{c}_{k\uparrow}^\dagger + \hat{c}_{k\downarrow}^\dagger \hat{c}_{j\uparrow}^\dagger) \\
&+ 2X_\alpha \sum_{\langle jk \rangle_\alpha} \left(\mathrm{e}^{\mathrm{i}Pj} - \mathrm{e}^{\mathrm{i}Pk}\right) \\
&\times \left((\hat{n}_{k\uparrow} - \hat{n}_{j\downarrow}) \hat{c}_{j\downarrow}^\dagger \hat{c}_{k\uparrow}^\dagger + (\hat{n}_{k\downarrow} - \hat{n}_{j\uparrow}) \hat{c}_{k\downarrow}^\dagger \hat{c}_{j\uparrow}^\dagger\right) \\
&+ \sum_{\langle jk \rangle_\alpha} \left(\frac{Y_\alpha}{2} \mathrm{e}^{\mathrm{i}Pj} - V_\alpha \mathrm{e}^{\mathrm{i}Pk}\right) (\hat{n}_j - 1) \hat{c}_{k\uparrow}^\dagger \hat{c}_{k\downarrow}^\dagger \\
&+ \sum_{\langle jk \rangle_\alpha} \left(\frac{Y_\alpha}{2} \mathrm{e}^{\mathrm{i}Pk} - V_\alpha \mathrm{e}^{\mathrm{i}Pj}\right) (\hat{n}_k - 1) \hat{c}_{j\uparrow}^\dagger \hat{c}_{j\downarrow}^\dagger \\
&- 2\mu \eta_P^\dagger. \qquad (6)
\end{aligned}$$

Using (6) one finds the conditions under which the $\eta-$pairing states (5) are eigenstates of H. For the momenta $P \in \{0, \pi\}$ we have the following constraints on the interaction constants:

$P = 0$	$P = \pi$
$X_\alpha = t_\alpha$	$X_2 = t_2$
$Y_\alpha = 2V_\alpha$	$Y_\alpha = (-1)^\alpha 2V_\alpha$

Note that for momentum $P = \pi$ no conditions relating t_1 to X_1 exist. In the following we shall only consider the $P = 0$ case. Other values of the momenta can be treated similarly. An investigation of the properties of these states can be found *e.g.* in [18].

In order to make the η-pairing state (with momentum $P = 0$) an optimum ground state we first observe that $|\eta\rangle$ can be built completely from the local 3-site states $|000\rangle$, $|222\rangle$, $|002\rangle + |200\rangle + |020\rangle$ and $|022\rangle + |220\rangle + |202\rangle$ and analogous 4-site states. Without next-nearest neighbour interactions all local states have the same local energy $e_0 = U/(2Z) + V$ if we set $\mu = 0$. Demanding that e_0 is the local ground state energy and hence all other local energies must be larger, one obtains the following inequalities:

$$\begin{aligned}
&V \leq 0, \\
&\frac{U}{Z} \leq \min\left\{\mathfrak{B}_1^{(n)}, \mathfrak{B}_2^{(n)}, \mathfrak{B}_3^{(n)}, \mathfrak{B}_4^{(n)}, \dots\right\} \quad (n = 3, 4)
\end{aligned}$$

$$\begin{aligned}
\mathfrak{B}_1^{(3,4)} &:= -2|t| - 2V \\
\mathfrak{B}_2^{(3,4)} &:= -V + \frac{J^z}{4} \\
\mathfrak{B}_3^{(3,4)} &:= -V + \frac{1}{8}\left(-J^z - \sqrt{(J^z)^2 + 8(J^{xy})^2}\right) \\
\mathfrak{B}_4^{(3)} &:= \frac{1}{3}\left(-5V - \frac{J^z}{4} - \frac{|J^{xy}|}{2}\right. \\
&\quad \left. -\frac{1}{4}\sqrt{(4V - J^z - 2|J^{xy}|)^2 + 192t^2}\right). \qquad (7)
\end{aligned}$$

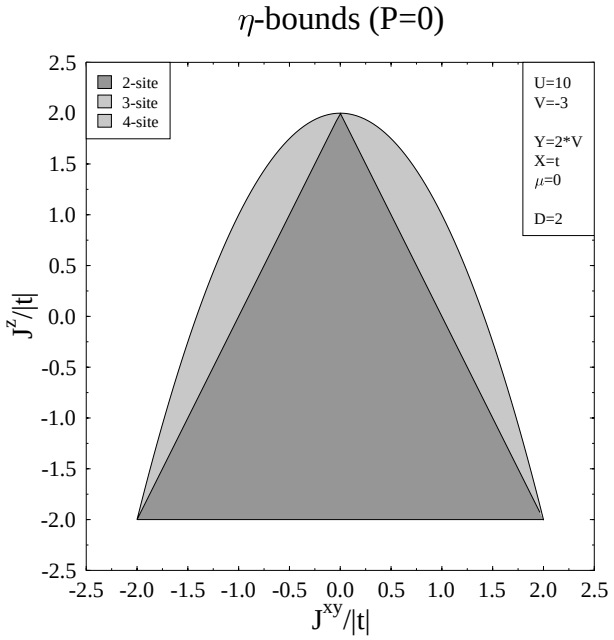

Fig. 2. Stability region of the η-pairing state with momentum $P = 0$ in the $J^z - J^{xy}$ cut in units of $|t|$ for different cluster sizes.

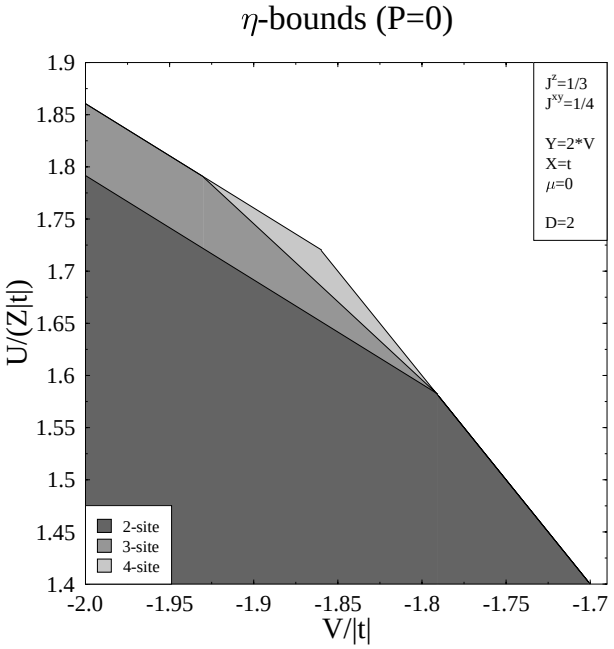

Fig. 3. A $U - V$ cut for the η-pairing state with momentum $P = 0$ in units of $|t|$.

These inequalities represent the stability regions for the η-pairing state with momentum $P = 0$. The selected[1] bounds $\mathfrak{B}_j^{(n)}$ belong to the *3*-site and/or *4*-site case and can be distinguished by the upper index n. There are seven bounds for $n = 3$ and more than 50 for $n = 4$. The first two bounds were also obtained by using the bond-diagonalization [12]. The other bounds are new and indicate an improvement of the stability region.

It is possible to investigate all cuts of the parameter space (t, U, V, J^z, J^{xy}), but we shall concentrate only on some of them. For all cuts we took realistic parameter values satisfying $U \geq V \geq t \geq J^z \geq J^{xy}$.

In the $J^z - J^{xy}$ cut of the parameter space (Fig. 2) the inner triangle corresponds to the stability region of the η-pairing state with momentum $P = 0$ obtained by bond-diagonalization. The enlargement corresponds to results achieved by the *3*-site Hamiltonian (including purely nearest neighbour interaction). The *4*-site Hamiltonian yields no further improvement of the bounds. However, it is not clear that the η-pairing state is not a ground state outside of those bounds since larger cluster sizes might yield a further enlargement of the stability region. In contrast to the last figure the following $U - V$ cut (Fig. 3) displays also an enhancement achieved by *4*-site diagonalization.

The inclusion of next-nearest neighbour interactions modifies the local ground state energy $e_0 = U/(2Z) + V_1 + V_2$ and hence the constraints concerning the interaction parameters:

$$
\begin{aligned}
& V_1 \leq -4V_2, \qquad \frac{U}{Z} \leq \min\{\mathfrak{B}_1, \mathfrak{B}_2, \mathfrak{B}_3, \mathfrak{B}_4, \dots\} \\
& \mathfrak{B}_1 := -V_1 - V_2 + \frac{1}{4}\left(J_1^z + J_2^z\right) \\
& \mathfrak{B}_2 := 2\left(-t_2 - V_1 - V_2 - \sqrt{(t_2+V_2)^2 + t_1^2}\right) \\
& \mathfrak{B}_3 := \frac{1}{8}\Big(-8\left(V_1+V_2\right) - J_1^z + 2J_2^{xy} \\
& \qquad -\sqrt{(J_1^z - 2J_2^z + 2J_2^{xy})^2 + 8(J_1^{xy})^2}\Big) \\
& \mathfrak{B}_4 := \frac{1}{3}\Big(-2|t_2| - 5\left(V_1+V_2\right) \\
& \qquad +\frac{1}{4}\left(J_1^z - 3J_2^z\right) + \frac{1}{2}\left(J_1^{xy} + 3J_2^{xy}\right)\Big) - \frac{1}{12} \\
& \times\sqrt{(-8|t_2| + 4(V_1+V_2) - J_1^z + 3J_2^z + 2J_1^{xy} - 6J_2^{xy})^2 + 192t_1^2}.
\end{aligned}
\tag{8}
$$

These bounds belong to the *3*-site diagonalization results since larger clusters cannot be diagonalized analytically in closed form. In order to be close to real systems we take smaller next-nearest neighbour parameters than corresponding nearest neighbour ones and express this through ratios $r_P := P_1/P_2$ with $P_\alpha \in \{t_\alpha, V_\alpha, J_\alpha^z, J_\alpha^{xy}\}$. The ratios depend on the material and hence can be very different. Since the η-pairing states with momentum $P = 0$ consist of electron pairs it is interesting to consider the $Y_1 - Y_2$ cut (Fig. 4). This cut represents the behaviour of the stability region for different on-site Coulomb interaction parameters U. All other parameter pairs have the same ratio $r_P = 3$. Note that on the square lattice the numbers of nearest and next-nearest neighbours are exactly the same. One important observation is that the two parameters Y_1 and Y_2 stabilize the ground state with increasing Coulomb repulsion ($U > 0$) which try to seperate the electron pairs. The fully polarized ferromagnetic state is a simple tensor

[1] We have listed in (4) only those bounds which are relevant for Figures 2 and 3. A complete list of the bounds $\mathfrak{B}_j^{(3)}$ can be found in the appendix. The bounds $\mathfrak{B}_j^{(4)}$ can be found in [20].

product of local states

$$|F\rangle = \prod_{i=1}^{L} \hat{c}_{i\uparrow}^{\dagger}|0\rangle, \tag{9}$$

where each lattice site is occupied by an electron with spin $\sigma = \uparrow$ (at half-filling[2]). In contrast to the η-pairing state this state is already an eigenstate of our Hamiltonian and hence there are no restrictions concerning the parameters. Nevertheless, we concentrate on the special case[3] $X = t$. If we want $|F\rangle$ to become an optimum ground state we have to make $|\sigma\sigma\sigma\rangle$ or $|\sigma\sigma\sigma\sigma\rangle$ the local ground state. Without next-nearest neighbour interaction the corresponding local energy $e_0 = -U/(2Z) + J^z/4 - 2\mu/Z$ is a lower bound for the other local energies leading to the inequalities:

$$\begin{aligned}
&J^z \leq -|J^{xy}|,\\
&\frac{U}{Z} \geq \max\left\{\mathfrak{B}_1^{(n)},\, \mathfrak{B}_2^{(n)},\, \mathfrak{B}_3^{(n)},\, \dots\right\} \quad (n = 3, 4)\\
&\mathfrak{B}_1^{(3,4)} := 2|t| + \frac{J^z}{2} + \frac{2|\mu|}{Z}\\
&\mathfrak{B}_2^{(3,4)} := -V + \frac{J^z}{4} - \frac{2|\mu|}{Z}\\
&\mathfrak{B}_3^{(3)} := \frac{1}{2}\left(V + \frac{J^z}{2} + \frac{|\mu|}{Z} + \sqrt{\left(V + \frac{|\mu|}{2}\right)^2 + 2Y^2}\right)\\
&\mathfrak{B}_3^{(4)} := \frac{1}{2}\left(V + \frac{J^z}{2} + \sqrt{V^2 + 2Y^2}\right).
\end{aligned} \tag{10}$$

The first two boundaries are the same as those of the bond-results [12], the last ones are new. Hence an improvement of the ground state region might be obtained by considering the last two bounds. But the number of all possible two dimensional cuts is still very large.

The bounds can be further improved using the following argument [12]. With a fixed particle number N a state is a ground state of H but also a ground state of $H + \mu N$. In this situation one can regard the bounds as a function of μ and try to find the value of μ which optimizes these bounds. For instance, if we have inequalities like $a \geq b + \mu$ and $a \geq c - \mu$ then the best value is $\mu = (c - b)/2$ and thus $a \geq (b + c)/2$. In our case we get $\mu = 0$ and therefore $\mathfrak{B}_3^{(3)} = \mathfrak{B}_3^{(4)}$. This leads to the cognition that only the 3-site diagonalization is necessary, and the inclusion of four local lattice sites does not improve the stability region. This result is shown in [20] for various two dimensional cuts of the parameter space. With next-nearest neighbour interaction parameters we get the modified local energy $e_0 = -U/(2Z) + J_1^z/4 + J_2^z/4$ with the corresponding

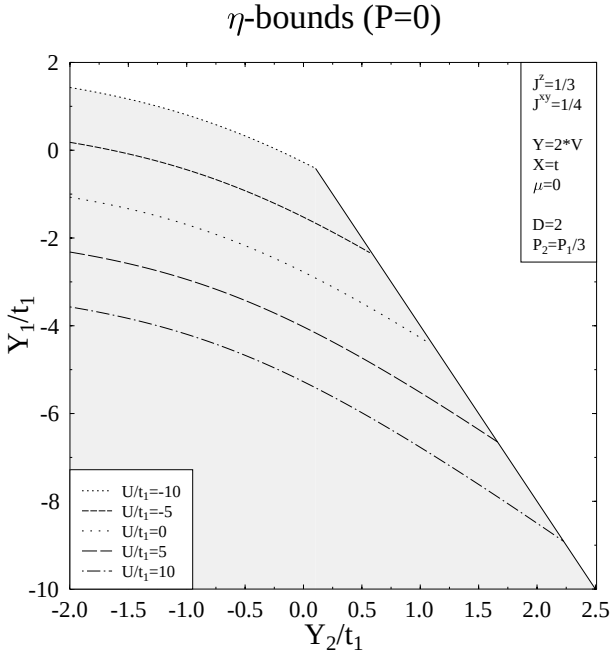

Fig. 4. A $Y_1 - Y_2$ cut for the bounds of the η-pairing state with momentum $P = 0$ with non-zero next-nearest neighbour interactions. The stability domains are shown for different values of U.

new inequalities:

$$\begin{aligned}
&J_1^z \leq -2\left(J_2^z + J_2^{xy}\right), \qquad (J_1^z)^2 - (J_1^{xy})^2 \leq -2\left(J_2^z - J_2^{xy}\right) J_1^z,\\
&\frac{U}{Z} \geq \max\left\{\mathfrak{B}_1,\, \mathfrak{B}_2,\, \mathfrak{B}_3,\, \mathfrak{B}_4, \dots\right\}\\
&\mathfrak{B}_1 := -V_1 - V_2 + \frac{1}{4}\left(J_1^z + J_2^z\right)\\
&\mathfrak{B}_2 := 2t_2 + \frac{1}{2}\left(J_1^z + J_2^z\right) + \frac{1}{2}\sqrt{\left(4t_2 + J_2^z\right)^2 + 16t_1^2}\\
&\mathfrak{B}_3 := \frac{1}{2}V_1 - \frac{1}{2}Y_2 + \frac{1}{4}\left(J_1^z + J_2^z\right)\\
&+ \frac{1}{2}\sqrt{\left(V_1 + Y_2\right)^2 + 2Y_1^2 - 4V_2\left(V_1 + Y_2 - V_2\right)}\\
&\mathfrak{B}_4 := 2t_2 + J_1^z + J_2^z - \frac{1}{2}\left(J_1^{xy} + J_2^{xy}\right) + \frac{1}{2}\\
&\times\sqrt{(4t_2 + J_2^{xy})^2 + (J_1^z - J_1^{xy})(J_1^z - J_1^{xy} + 2J_2^{xy} + 8t_2) + 16t_1^2}.
\end{aligned} \tag{11}$$

The pure Hubbard model $H = H(t_1, U)$ exhibits no ferromagnetic ground state at half-filling. Only for some special cases like the Nagaoka case [21] the existence of a fully polarized ferromagnetic ground state can be proven. An extension to the case of the generalized Hubbard model can be found in [22]. The influence of long range hopping t_α on ferromagnetism (at half-filling) was investigated *e.g.* by Farkašovský [23]. The results show a suppression of ferromagnetism with increasing α. In the $U - t_1$ cut (Fig. 5) we considered the behaviour of the stability region for different t_2 values. But in contrast to [23] all other type of couplings were not turned off. The inclusion of the next-nearest neighbour hopping shows a reduction of the stability region for the ferromagnetic ground state in agreement with the results of [23].

[2] Away from half-filling the ferromagnetic state is no optimum ground state.

[3] For $X \neq t$ one has to rely on numerical methods. Preliminary results show a behaviour similar to the case $X = t$.

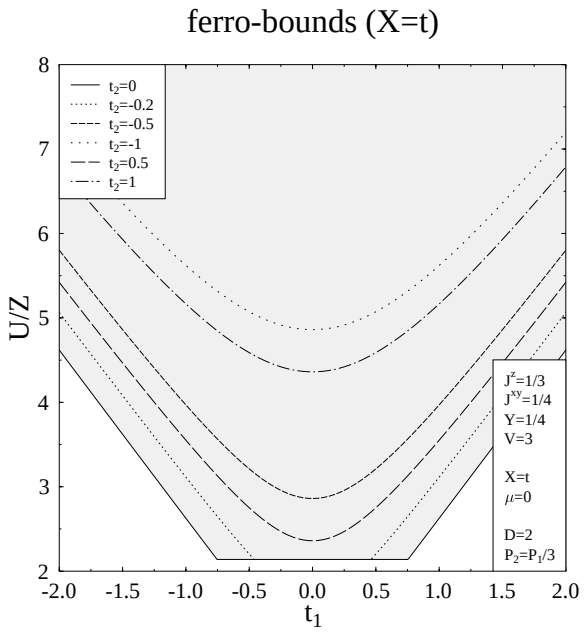

Fig. 5. Bounds for the stability region of the ferromagnetic state in the $U-t_1$ plane for different values of the next-nearest neighbour hopping t_2.

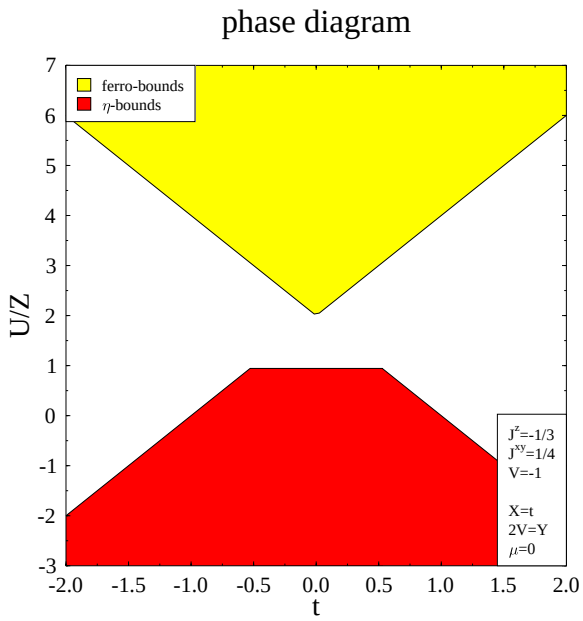

Fig. 6. Phase diagram of the generalized Hubbard model with nearest neighbour interactions only.

5 Conclusions

We have presented exact results for stability regions of two physically interesting ground states of the generalized Hubbard model with nearest and next-nearest neighbour interaction using the optimum ground state approach. First we looked at the η-pairing state with momentum $P = 0$ and then at the fully polarized ferromagnetic state at half-filling. We have studied the behaviour of the stability domains of these two states with increasing cluster size. But due to difficulties that emerge for analytical diagonalization, we have limited our analytical calculations to two cluster sizes, *i.e.* $N(\square) = \{3, 4\}$. These cluster Hamiltonians were divided into bond Hamiltonians so that a comparison with results obtained by bond diagonalization [12] was possible. The new boundaries which exhibit an improvement were illustrated graphically in some chosen cuts of the parameter space. Without next-nearest neighbour interactions all cuts show an enlargement of the stability domains obtained by *3*-site diagonalization. The extension to four lattice sites only have led to an amplification in the $U-V$ cut, and all other cuts indicated a fast convergence of the stability regions. We expect that any further improvement is rapidly decreasing with increasing cluster size. Another aim of this work was to determine the effects of next-nearest neighbour interactions on the stability domains. However, we restricted our investigation to the *3*-site case only. The illustration of these bounds indicates that the stability conditions are strongly dependent on the next-nearest neighbour parameters. For instance, in the ferromagnetic case one finds a reduction of the stability domain ($U-t_1$ cut) in the presence of next-nearest neighbour hopping t_2. In the case of the η-pairing state with momentum $P = 0$ we considered the $Y_1 - Y_2$ cut for different values of the on-site Coulomb interaction U. With increasing Coulomb repulsion ($U > 0$) which tries to separate the electron pairs we observed a stabilization of the domain because of large negative Y_1 values.

In summary, we have shown that a cluster of three and four lattice sites can be treated (with some restrictions) analytically whereby every two-dimensional cut of the whole parameter space can immediately be examined and does not require long numerical calculations. Although we restricted ourselves mainly to the case $X = t$, where the local Hamiltonian decays into small blocks which can be diagonalized in closed form, we like to stress that the optimum ground state approach can be used to treat the general case $X \neq t$ as well. Here one can either diagonalize the larger block matrices numerically [14] or combine the optimum ground state method with the Gerschgorin approach of [10]. Instead of determining the eigenvalues of the larger matrices exactly one can obtain lower bounds in closed form by using Gerschgorin's theorem. Although these bounds will in general not be the best possible ones they still yield exact stability regions for the state under consideration. The results give valuable information about the phase diagram. In Figure 6 the stability regions of the two states investigated here are shown for a generalized Hubbard model with only nearest neighbour interactions. For the parameter values chosen one already knows a considerable part of the phase diagram. These results might serve as a guidance for further computer simulations or exact diagonalization studies. Apart from this aspect, the extension enables some interesting new investigations due to the inclusion of more correlations.

We like to thank Jan de Boer and Zsolt Szabó for helpful discussions.

Appendix

To obtain an optimum ground state for a given system one has to determine all local eigenvalues. For instance, in the 3-site case (with $\mu = 0$, $X_\alpha = t_\alpha$ and next-nearest neighbour interaction) the eigenvalues have the form:

$$
\begin{aligned}
e_1 &:= \frac{U}{2Z} + V_1 + V_2,\\
e_2 &:= -\frac{U}{2Z} + \frac{J_1^z}{4} + \frac{J_2^z}{4},\\
e_3 &:= \frac{U}{4Z} + t_2 + \frac{V_1}{2},\\
e_4 &:= \frac{U}{2Z} - V_2 - Y_2,\\
e_5 &:= -\frac{U}{4Z} + t_2 + \frac{J_1^z}{8},\\
e_6 &:= -\frac{U}{2Z} - \frac{J_2^z}{4} - \frac{J_2^{xy}}{2},\\
e_{7,8} &:= -\frac{U}{4Z} \pm t_2 - \frac{J_1^z}{8} \pm \frac{J_1^{xy}}{4},\\
e_9 &:= \frac{U}{2Z} - \frac{V_1}{2} + \frac{Y_2}{2}\\
&\quad - \frac{1}{2}\sqrt{(V_1 - 2V_2 + Y_2)^2 + 2Y_1^2},\\
e_{10} &:= -\frac{U}{2Z} - \frac{J_1^z}{8} + \frac{J_2^{xy}}{4}\\
&- \frac{1}{8}\sqrt{(J_1^z - 2J_2^z + 2J_2^{xy})^2 + 8(J_1^{xy})^2},\\
e_{11} &:= \frac{U}{8Z} - \frac{t_2}{2} + \frac{V_1}{4} + \frac{V_2}{2}\\
&- \frac{1}{8}\sqrt{\left(-\frac{U}{Z} + 4t_2 - 2V_1 + 4V_2\right)^2 + 32t_1^2},\\
e_{12} &:= -\frac{U}{8Z} - \frac{t_2}{2} + \frac{J_1^z}{16} + \frac{J_2^z}{8}\\
&- \frac{1}{16}\sqrt{\left(\frac{2U}{Z} + 8t_2 - J_1^z + 2J_2^z\right)^2 + 128t_1^2},\\
e_{13,14} &:= -\frac{U}{8Z} \mp \frac{t_2}{2} - \frac{J_1^z}{16} - \frac{J_2^z}{8} \pm \frac{J_1^{xy}}{8} \pm \frac{J_2^{xy}}{4}\\
&- \frac{1}{16}\sqrt{\left(\pm\frac{2U}{Z} + 8t_2 \pm J_1^z \mp 2J_2^z - 2J_1^{xy} + 4J_2^{xy}\right)^2 + 128t_1^2},\\
e_{15,16} &:= 2\Omega\cos\left(\frac{\theta}{3}\right) - \frac{1}{3}\left(\frac{U}{4Z} \pm 2t_2 \mp Y_2 - \frac{V_1}{2} - V_2\right),\\
e_{17,18} &:= 2\Omega\cos\left(\frac{\theta + 2\pi}{3}\right)\\
&- \frac{1}{3}\left(\frac{U}{4Z} \pm 2t_2 \mp Y_2 - \frac{V_1}{2} - V_2\right),\\
e_{19,20} &:= 2\Omega\cos\left(\frac{\theta + 4\pi}{3}\right)\\
&- \frac{1}{3}\left(\frac{U}{4Z} \pm 2t_2 \mp Y_2 - \frac{V_1}{2} - V_2\right).
\end{aligned}
$$

The expressions of the functions Ω and θ, which include the interaction terms, are to large and hence are omitted.

The bounds are derived from the inequalities $e_0 \le e_i$ (for all i). For the η-paring state with $P = 0$ one has $e_0^{(\eta)} = e_1$. It becomes an optimum ground state if the conditions $V \le 0$ and $U/Z \le \min\{\mathfrak{B}_1, \ldots, \mathfrak{B}_7\}$ are satisfied, where

$$
\begin{aligned}
\mathfrak{B}_1^{(3)} &= -2|t| - 2V,\\
\mathfrak{B}_2^{(3)} &= -V + \frac{J^z}{4},\\
\mathfrak{B}_3^{(3)} &= -V - \frac{J^z}{8} - \frac{1}{8}\sqrt{(J^z)^2 + 8(J^{xy})^2},\\
\mathfrak{B}_4^{(3)} &= \frac{1}{3}\left(-5V - \frac{J^z}{4} - \frac{|J^{xy}|}{2}\right.\\
&\quad \left. -\frac{1}{4}\sqrt{(4V - J^z - 2|J^{xy}|)^2 + 192t^2}\right),\\
\mathfrak{B}_5^{(3)} &= \frac{1}{6}\left(-8V + J^z\right),\\
\mathfrak{B}_6^{(3)} &= \frac{1}{6}\left(-8V - J^z + 2|J^{xy}|\right),\\
\mathfrak{B}_7^{(3)} &= \frac{1}{3}\left(-5V - \frac{J^z}{4} - \frac{1}{4}\sqrt{(4V + J^z)^2 + 192t^2}\right).
\end{aligned}
$$

Due to the complexity of the last six eigenvalues (e_{15} - e_{20}) the corresponding bounds do not exist in "closed form", but numerical investigations show that they are irrelevant. Including also next-nearest neighbour terms one gets:

$$
\begin{aligned}
\mathfrak{B}_1 &= -V_1 - V_2 + \frac{1}{4}(J_1^z + J_2^z),\\
\mathfrak{B}_2 &= 2\left(-t_2 - V_1 - V_2 - \sqrt{(t_2 + V_2)^2 + t_1^2}\right),\\
\mathfrak{B}_3 &= \frac{1}{8}\left(-8(V_1 + V_2) - J_1^z + 2J_2^{xy}\right.\\
&\quad \left. - \sqrt{(J_1^z - 2J_2^z + 2J_2^{xy})^2 + 8(J_1^{xy})^2}\right),\\
\mathfrak{B}_4 &= -\frac{2t_2}{3} - \frac{5}{3}(V_1 + V_2)\\
&\quad - \frac{1}{12}(J_1^z + 3J_2^z) + \frac{1}{6}(J_1^{xy} + 3J_2^{xy}) - \frac{1}{12}\\
&\times\sqrt{(8t_2 - 4(V_1 + V_2) + J_1^z - 3J_2^z - 2J_1^{xy} + 6J_2^{xy})^2 + 192t_1^2},\\
\mathfrak{B}_5 &= \frac{2t_2}{3} - \frac{5}{3}(V_1 + V_2) - \frac{1}{12}(J_1^z + 3J_2^z) - \frac{1}{6}(J_1^{xy} + 3J_2^{xy}) - \frac{1}{12}\\
&\times\sqrt{(8t_2 + 4(V_1 + V_2) - J_1^z + 3J_2^z - 2J_1^{xy} + 6J_2^{xy})^2 + 192t_1^2},\\
\mathfrak{B}_6 &= 4t_2 - 2V_1 - 4V_2,\\
\mathfrak{B}_7 &= -V_1 - V_2 - \frac{1}{4}(J_2^z + 2J_2^{xy}),\\
\mathfrak{B}_8 &= -\frac{1}{6}(-8t_2 + 8V_1 + 8V_2 - J_1^z),\\
\mathfrak{B}_9 &= -\frac{1}{6}(8|t_2| + 8V_1 + 8V_2 + J_1^z + 2|J_1^{xy}|),\\
\mathfrak{B}_{10} &= -\frac{2t_2}{3} - \frac{5}{3}(V_1 + V_2) + \frac{J_1^z}{12} + \frac{J_2^z}{4}\\
&\quad - \frac{1}{12}\sqrt{(-8t_2 + 4(V_1 + V_2) + J_1^z - 3J_2^z)^2 + 192t_1^2}.
\end{aligned}
$$

The ferromagnetic state has $e_0^{(\mathrm{F})} = e_2$ and the corresponding bounds can be derived in an analogous way.

The number of eigenvalues and bounds in the case $n = 4$ is too large to be listed here. They can be found in [20].

References

1. J. Hubbard, Proc. R. Soc. London A **276**, 238 (1963).
2. M.C. Gutzwiller, Phys. Rev. Lett. **10**, 159 (1963).
3. J. Kanamori, Prog. Thoer. Phys. **30**, 275 (1963).
4. E.H. Lieb, F.Y. Wu, Phys. Rev. Lett. **17**, 1133 (1966).
5. W. Metzner, D. Vollhardt, Phys. Rev. Lett. **62**, 324 (1989).
6. E. Müller-Hartmann, Z. Phys. B **74**, 507 (1989).
7. U. Brandt, A. Giesekus, Phys. Rev. Lett. **68**, 2648 (1992).
8. R. Strack, D. Vollhardt, Phys. Rev. Lett. **70**, 2637 (1993).
9. R. Strack, D. Vollhardt, Phys. Rev. Lett. **72**, 3425 (1994).
10. A.A. Ovchinnikov, J. Phys. CM **6**, 11057 (1994).
11. J. de Boer, V.E. Korepin, A. Schadschneider, Phys. Rev. Lett. **74**, 789 (1995).
12. J. de Boer, A. Schadschneider, Phys. Rev. Lett. **75**, 4298 (1995).
13. A. Klümper, A. Schadschneider, J. Zittartz, Europhys. Lett. **24**, 293 (1993).
14. Z. Szabó, Phys. Rev. B **59**, 10007 (1999).
15. J.E. Hirsch, Phys. Lett. A **134**, 451 (1989).
16. S. Kivelson, W.P. Su, J.R. Schrieffer, A.J. Heeger, Phys. Rev. Lett. **58**, 1899 (1987).
17. K.A. Penson, M. Kolb, Phys. Rev. B **33**, 1663 (1986).
18. A. Schadschneider, Phys. Rev. B **51**, 10386 (1995).
19. C.N. Yang, Phys. Rev. Lett. **63**, 2144 (1989).
20. C. Dziurzik, Diplomarbeit, Universität zu Köln (1998).
21. Y. Nagaoka, Solid State Comm. **3**, 409 (1965).
22. M. Kollar, R. Strack, D. Vollhardt, Phys. Rev. B **53**, 9225 (1996).
23. P. Farkašovský, Int. J. Mod. Phys. B **12**, 803 (1997).